

5. Further Aspects and Conclusions

In a previous work it was shown that the scavenging efficiency of DMD for radicals depends on the excess of DMD over the radicals [4]. This is still more critical when scavenging flame radicals. The curves of Fig. 1 show that for certain radicals, e.g. phenyl, an excess of about 10^6 is necessary to suppress the loss of radicals by other reactions. In these cases it is not so much the excess over the radical concentration that is important, but that over other reactants, for example unsaturated hydrocarbons, with which the radicals can also react when they condense together.

The use of a cooled plane plate having only a low rim is not yet satisfactory with respect to the scavenging and condensation efficiency. If one compares the number of aromatic molecules (e.g. naphthalene, ethynyl benzene, etc.) condensing per time on the plate with their inflow through the nozzle, calculated on account of their mole fraction in the flame as determined by other methods, one obtains a condensing efficiency of only about 2%. The reason for this is probably the relatively high velocity of the molecules in the beam and a comparatively broad beam when sampling from a high temperature source. The collecting device is therefore reconstructed with the aim to reach a scavenging or condensing efficiency, respectively, much nearer to one. If this could be accomplished the method would be nearly independent of calibration methods for radicals.

These experiments which must still be regarded as preliminary have shown that it is possible to scavenge large radicals from flames and other low-pressure reaction systems by reaction with DMD in the condensed phase. On the other hand can the analysis of stable trace components (e.g. polycyclic aromatic hydrocarbons) be put on more solid grounds by comparing the composition of samples drawn with and without a radical scavenger. The method inevitably needs sampling and suffers therefore from the notorious disadvantages connected with it. It is not suitable for every radical, for example not for H atoms and radicals that give unspecific scavenging products. Different radicals, in particular carbenes, react in a different way with the scavenger and it is necessary to study different types of reactions with

DMD in separate experiments. The example of phenyl has shown that it can be usefully applied to medium sized monoradicals which react with DMD in a simple and unequivocal manner. An improvement of the method by changing some constructional details is being undertaken.

The support of this work by the Deutsche Forschungsgemeinschaft, by the Stiftung Volkswagenwerk and by the Fonds der Chemischen Industrie is gratefully acknowledged.

References

- [1] Th. Just, Ber. Bunsenges. Phys. Chem. 87, 968 (1983).
- [2] J. A. Cole, J. D. Bittner, J. P. Longwell, and J. B. Howard, Combust. Flame 56, 51 (1984).
- [3] O. I. Smith and D. W. Chandler, Combust. Flame 63, 19 (1986).
- [4] M. Schottler and K. H. Homann, Ber. Bunsenges. Phys. Chem. 91, 688 (1987).
- [5] K. H. Homann, W. Lange, and H. Gg. Wagner, Ber. Bunsenges. Phys. Chem. 75, 121 (1971).
- [6] H. W. Wenz, Dissertation, TH Darmstadt D17 (1983); H. Bockhorn, F. Fetting, and H. W. Wenz, Ber. Bunsenges. Phys. Chem. 87, 1067 (1983).
- [7] K. H. Homann and H. Gg. Wagner, Ber. Bunsenges. Phys. Chem. 69, 20 (1965).
- [8] J.-L. Delfau and Ch. Vovelle, J. Chim. Phys. Phys.-Chim. Biol. 82, 747 (1985).
- [9] P. R. Westmoreland, MIT, PhD Thesis, Massachusetts 1986.
- [10] M. Schottler, Dissertation D17, TH Darmstadt 1986.
- [11] E. Kovats, Helv. Chim. Acta 41, 1915 (1958); A. Wehrli and E. Kovats, Helv. Chim. Acta 42, 2709 (1959); R. Kaiser, Chromatographie in der Gasphase, Vol. III, Bibliographisches Institut, Mannheim 1962; G. Schomburg, J. Chromatogr. 23, 1 (1966).
- [12] H. Brachhold, Dissertation D17, TH Darmstadt 1987.
- [13] F. LeGoff and B. Vuilleumoz, J. Chim. Phys. Physicochim. Biol. 66, 403 (1969).
- [14] M. McCarty Jr. and G. W. Robinson, J. Chim. Phys. 56, 723 (1959).
- [15] K. H. Homann and H. Schweinfurth, Ber. Bunsenges. Phys. Chem. 85, 569 (1981).
- [16] M. Schottler, Diplomarbeit, TH Darmstadt 1982.
- [17] A. Heddrich, Dissertation D17, TH Darmstadt 1986.
- [18] W. A. Pryor and H. Guard, J. Am. Chem. Soc. 86, 1150 (1964).
- [19] T. Toth, J. Chromatogr. 279, 157 (1983).

(Eingegangen am 12. März 1987)

E 6462

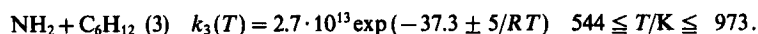
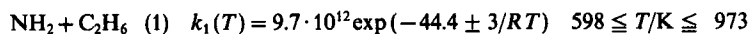
Hydrogen Abstraction Reactions by $\text{NH}_2(\tilde{\text{X}}^2\text{B}_1)$ -Radicals from Hydrocarbons in the Gas Phase

J. Ehbrecht, W. Hack, P. Rouveirolles*), and H. Gg. Wagner

Max-Planck-Institut für Strömungsforschung, Bunsenstrasse 10, D-3400 Göttingen, W.-Germany

Elementary Reactions / Radicals

Rate constants for the reactions of the $\text{NH}_2(\tilde{\text{X}}^2\text{B}_1)$ radical with ethane, propane and cyclohexane were measured in an isothermal flow system. Kinetic data were obtained at 4 mbar helium pressure in the high temperature range given below. $[\text{NH}_2](t)$ -profiles were mapped at pseudo-first order conditions $[\text{NH}_2]_0 \ll [\text{RH}]_0$ with the laser induced fluorescence technique. The temperature dependence of the rate constants is represented by the following Arrhenius-expressions: A in $[\text{cm}^3/\text{mol} \cdot \text{s}]$ and E_A in $[\text{kJ/mol}]$:



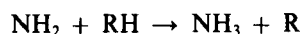
A correlation of the activation energy with the energy of the broken C-H bond of various hydrocarbons is discussed.

*) Permanent address: CNRS, CRCCHT, Orleans.

Introduction

The amino radical $\text{NH}_2(\tilde{X}^2\text{B}_1)$ is an important intermediate species in the combustion chemistry of ammonia and N-containing fuels. Detailed models of hydrocarbon-air flames and the chemistry of the earth's atmosphere require the knowledge of the appropriate rate constants of NH_2 elementary reactions. In particular in technical combustion NH_2 reactions with hydrocarbons at high temperatures are of great interest because NH_2 , which is admixed in combustion processes for eliminating nitric oxides [1] could react with hydrocarbons at these temperatures.

Hydrogen abstraction reactions with ethane, propane, n-butane and iso-butane of the type:



were measured in laser photolysis experiments at low temperatures [2] and, moreover, rate constants for these reactions were calculated from data of shock tube experiments [3]. Heating the flow reactor via a silver furnace measurements with methane [4], iso-butane, acetaldehyde, 2,2-dimethylpropane and toluene [5] were realized up to 1000 K, so that the interesting temperature range between laser photolysis and shock tube experiments can now be covered.

A relation between the Arrhenius activation energy and the energy of the broken C–H bond [6] can be established for a series of NH_2 reactions with hydrocarbons. This relation is clear for those hydrocarbons having only primary or secondary C atoms, so that there is only one path for hydrogen abstraction.

Reaction rates for the NH_2 radical with methane and 2,2-dimethylpropane in the medium temperature range have been presented [4, 5] as another hydrocarbon with only primary C atoms ethane was chosen for this work. With only secondary C atoms there is only one class of hydrocarbons, the cycloalkanes. Cyclohexane was chosen for this work, because the ring is, contrary to other lower cycloalkanes, nearly free of tension. Moreover the reaction with propane having both types of C atoms was measured.

A discharge flow system can be extended to study elementary reactions up to temperatures above 1000 K, limited by heterogeneous reactions. At these temperatures the fast reaction of ammonia with F atoms can still be used as an NH_2 radical source, if the contact of F atoms with the heated wall is avoided. The $\text{NH}_2(\tilde{X}^2\text{B}_1)$ radicals can still be detected by the specific laser induced fluorescence (LIF) technique with high sensitivity, if the NH_2 containing gas is cooled to room temperature in the detection volume.

The reactions:



with hydrocarbons containing primary H atoms (C_2H_6) or secondary H atoms (C_6H_{12}) are of special interest, since they allow to pin down the reactivity of these H atoms. These reactions were not yet studied directly in the intermediate

temperature range. Moreover for the reaction with cyclohexane no direct determinations for the rate are described in the literature.

The purpose of this work was to measure the temperature dependence of the reaction rates of reaction (1), (2) and (3) in the intermediate temperature range with a direct technique. Including former experiments a wide range of C–H bond energies is thus covered.

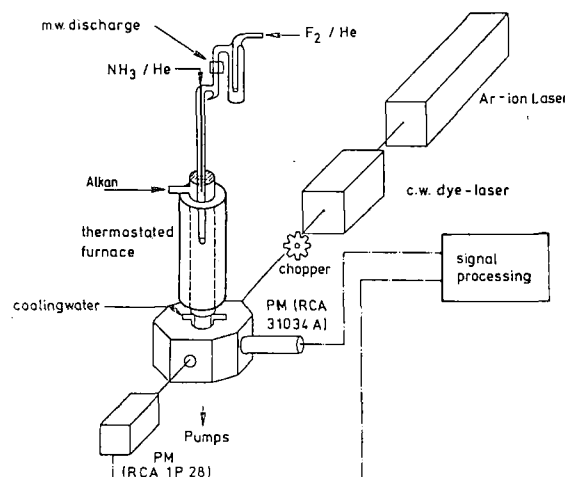


Fig. 1
Experimental arrangement

Experimental

The experimental arrangement used in this study is shown in Fig. 1. Some parts of it and the method of analysis have been described elsewhere [7], so only the principal characteristics and some modifications are given here.

Kinetic measurements have been carried out in an isothermal quartz flow reactor ($S/V = 0.70 \text{ cm}^{-1}$), inner diameter $\theta = 5.5 \text{ cm}$. In all experiments He was the main carrier gas. The flow velocity varied between 1.2 m/s and 1.4 m/s, and the temperature between 544 K and 1073 K. The pressure in the reactor was in all experiments 4 mbar. The reactor was directly connected to the fluorescence cell via a glass skimner. Two coaxial silver cylinders (2 and 5 mm thick) thermostated by electrical heating bandages covered the surface of the reactor, thermal insulation was achieved with Refrasil-batt (Chemical and Insulating, B-A3H). The temperature was measured directly on the surface of the reactor with three Ni–NiCr thermocouples serving simultaneously to control the temperature. In an independent experiment at $T = 945 \text{ K}$, in which a thermocouple was moved along the axis of the reactor, a relative error in the temperature profile of $\Delta T/T < 3\%$ was obtained. The gas stream was cooled down to room temperature before it entered the fluorescence cell.

NH_2 radicals were prepared in a movable probe (outer diameter $d = 2.2 \text{ cm}$), by means of the fast reaction:



The reaction proceeded under conditions where all F atoms were consumed in the probe, where $[\text{NH}_3]_0 \gg [\text{F}]_0$, so that no formation of NH was observed, and where $[\text{NH}_3][\text{HF}] < 10^{-20} [\text{mol}^2/\text{cm}^6]$, to avoid the formation of $\text{NH}_4\text{F(s)}$. F atoms were generated in an electrodeless microwave discharge in a F_2/He mixture. The NH_3/He mixture was introduced through the inner tube of the probe.

A small portion of the gas mixture entered the fluorescence cell through a glass skimner. The pressure in the fluorescence cell could be adjusted independent of the flow system with a roots-pump. It was kept at $p = 0.4 \text{ mbar}$ in all experiments.

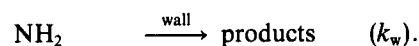
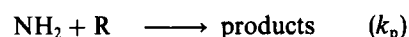
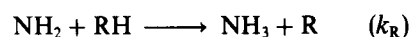
$\text{NH}_2(\tilde{X}^2\text{B}_1)$ radicals were detected by laser induced fluorescence (LIF) [8]. The $\text{NH}_2(\tilde{X}^2\text{B}_1)$ radicals were excited at $\lambda = 597.7 \text{ nm}$

($\tilde{\text{A}}^2\text{A}_1(0,9,0) - \tilde{\text{X}}^2\text{B}_1(0,0,0)$) by a cw-dye laser (Coherent 490) pumped by an Ar-ion laser (Spectra Physics Model 170). The integral fluorescence was observed perpendicular to the beam with a photomultiplier (RCA-(31034A01)) via a lock-in-amplifier-chart recorder combination.

Gases of highest commercially available purity were used without further purification. The F_2/He -mixture however was purified by passing it through three successive liquid N_2 traps and a NaF trap. Gas flows were measured with Tylan flow meters. Liquid reagents were controlled via saturators. The reactor walls were accurately cleaned with dilute HF and rinsed with distilled water. The cooled part of the reactor was coated with Teflon-varnish (Du Pont FEP 856-200).

Data Analysis

All experiments were carried out under pseudo-first order conditions ($[\text{RH}]_0 \gg [\text{NH}_2]_0$). NH_2 radicals were consumed according the reaction scheme:



The following differential equation describes the NH_2 radical depletion

$$-\text{d}[\text{NH}_2]/\text{d}t = k_{\text{w}}[\text{NH}_2] + k_{\text{R}}[\text{NH}_2][\text{RH}] + k_{\text{p}}[\text{NH}_2][\text{R}].$$

Under the experimental conditions applied and with the assumption of stationary $[\text{R}]$ -concentration this leads to:

$$-\text{d}[\text{NH}_2]/\text{d}t = k_{\text{ex}}[\text{NH}_2].$$

The experimentally determined rate constant k_{ex} counts for all different pathways consuming NH_2 radicals.

Assuming that the wall activity does not change when adding the reactant, the effective rate constant k_{eff} is obtained by subtracting k_{w} from k_{ex} :

$$k_{\text{ex}} - k_{\text{w}} = k_{\text{eff}} = k_{\text{R}}[\text{RH}] + k_{\text{p}}[\text{R}].$$

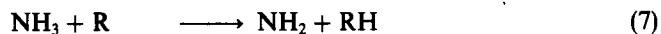
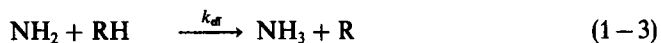
The limitations for the above given assumption are described for example in [7]. For k_{eff} only those values were taken into consideration for which the condition $k_{\text{eff}} > k_{\text{w}}$ was found (see discussion section). To account for all side reactions, k_{eff} is divided by a stoichiometric factor f obtained from computer simulations (see next part). From a plot of the corrected k_{eff} -values against the hydrocarbon concentration the rate constants k_{R} were determined.

A least-square treatment of the data provided the temperature dependance of the rate constants; standard errors for the activation energies were calculated the same way and apply to a 95% confidence interval.

Computation of the Stoichiometric Factors

As described above (see data analysis) the effective rate constant k_{eff} contains reactions by the products of the examined initial steps. Stoichiometric factors f were used to

correct this influence. They are obtained from a computer simulation taking the following reaction mechanism into account:



For k_{eff} (1–3) the uncorrected rate constants measured directly in the experiment were used. For k_{w} the experimental values obtained in each run were inserted. The rate constant for reaction (9) was estimated to be $k = 20 \text{ s}^{-1}$. The rate for reaction (7) was calculated from the reverse reaction. The rate constants for reactions (5, 6) have been reported [9,10] for $\text{R} = \text{C}_2\text{H}_5$ and C_3H_7 at $T = 298 \text{ K}$ and $p = 4 \text{ mbar}$. No temperature dependance has been assumed for these rate constants, moreover, the same values were used for ethane and cyclohexane. The initial NH_2 concentration was estimated.

The calculated $[\text{NH}_2](t)$ profiles yield a rate constant k'_{eff} , which is always larger than the inserted experimental value k_{eff} . The stoichiometric factor f is then calculated via:

$$f \equiv k'_{\text{eff}}/k_{\text{eff}}.$$

At the experimental conditions of this work it was found that the hydrogen abstraction pathway (1–3) was the main reaction channel. Accordingly, the stoichiometric factors f were found to be close to unity, i.e. in the range $1.01 < f < 1.23$. In additional tests it was found that the stoichiometric factors f are not very sensitive to variations of the rate constants of the reactions (5,6,9) and the initial NH_2 concentration. If in these tests k_5 , k_6 and k_9 were varied by a factor of 2, it was found that the greatest possible deviation of f was 8% (reaction (1) at $T = 598 \text{ K}$ for $f = 1.23$), for smaller values of f , the deviation is also smaller. The stoichiometric factors f calculated for each experiment are listed in the Tables 1–3.

Results

The experimental results for C_2H_6 , C_3H_8 and C_6H_{12} were obtained in independent experiments, details for each reactant are described.

The Reaction of Amino Radicals with Ethane

The temperature dependance of the rate constants for the reaction of NH_2 with C_2H_6 :



was studied over the temperature range $598 \leq T/\text{K} \leq 973$ at a pressure of $p = 4 \text{ mbar}$, under pseudo-first order conditions of a large excess of $[\text{C}_2\text{H}_6]_0$ over $[\text{NH}_2]_0$ ($8 \cdot 10^2 \leq [\text{C}_2\text{H}_6]_0/[\text{NH}_2]_0 \leq 1.6 \cdot 10^4$). The results and experimental details of 19 runs are

Table 1
Experimental conditions and results for reaction (1)

T [K]	$[\text{NH}_2]_0 \cdot 10^{12}$ [mol/cm ³]	$\frac{[\text{NH}_3]}{[\text{F}_2]}$	$[\text{C}_2\text{H}_6]_0 \cdot 10^3$ [mol/cm ³]	$\frac{[\text{C}_2\text{H}_6]_0}{[\text{NH}_2]_0}$	k_w [s ⁻¹]	k_{ex} [s ⁻¹]	f
598	1.34	66	10.7	8000	13.2	32.4	1.20
598	1.34	66	15.9	11900	13.2	44.7	1.22
598	1.34	66	21.4	15700	13.2	49.2	1.20
630	0.96	59	6.37	6700	17.9	37.1	1.17
630	0.96	59	9.54	10000	17.9	42.9	1.17
630	0.96	59	13.8	14400	17.9	53.3	1.15
673	1.41	56	8.61	6100	13.1	42.5	1.21
673	1.42	56	13.0	9200	13.1	59.6	1.19
673	1.42	56	17.1	12000	13.1	82.3	1.17
743	1.16	55	3.20	2800	22.3	54.3	1.16
743	1.16	55	6.39	5500	22.3	72.5	1.15
743	1.16	55	9.60	8300	22.3	104.7	1.13
743	1.16	55	12.8	11000	22.3	123.7	1.11
823	0.89	64	2.25	2500	26.0	67.0	1.14
823	0.89	64	3.67	4100	26.0	92.7	1.11
823	0.89	64	5.45	6100	26.0	111.1	1.10
973	0.95	58	0.70	800	16.0	51.5	1.16
973	0.95	58	1.33	1400	16.0	77.8	1.17
973	0.95	58	2.88	3000	16.0	148.7	1.08

Table 2
Experimental conditions and results for reaction (2)

T [K]	$[\text{NH}_2]_0 \cdot 10^{12}$ [mol/cm ³]	$[\text{NH}_3]_0 \cdot 10^{-11}$ [mol/cm ³]	$\frac{[\text{NH}_3]_0}{[\text{NH}_2]_0}$	$[\text{C}_3\text{H}_8]_0 \cdot 10^{-9}$ [mol/cm ³]	$\frac{10^3 [\text{C}_3\text{H}_8]_0}{[\text{NH}_2]_0}$	k_w [s ⁻¹]	k_{ex} [s ⁻¹]	f
550	0.93	6.55	70.4	17.02	18300	17.6	44.2	1.09
550	0.93	6.55	70.4	18.43	19817	17.6	51.9	1.08
550	0.93	6.55	70.4	20.76	22323	17.6	49.3	1.08
600	1.0	6.15	61.5	7.37	7370	22.2	49.4	1.07
600	1.0	6.15	61.5	9.33	9330	22.2	51.9	1.08
673	0.77	6.15	79.9	6.89	8948	11.0	71.9	1.04
673	0.77	6.15	79.9	8.12	10545	11.0	74.9	1.04
673	0.77	6.15	79.9	8.93	11597	11.0	80.7	1.04
673	0.77	6.15	79.9	10.19	13234	11.0	101.5	1.04
773	1.05	5.95	56.7	2.62	2495	32.5	81.0	1.04
773	1.05	5.95	57.7	3.75	3572	32.5	111.5	1.03
773	1.05	5.95	56.7	4.67	4448	32.5	127.0	1.03
873	0.88	5.92	67.3	0.73	829	26.5	54.1	1.03
873	0.88	5.92	7.3	1.27	1443	26.5	70.4	1.03
873	0.88	5.92	67.3	2.27	2579	26.5	92.7	1.03
973	0.91	6.54	71.9	0.59	648	30.8	73.6	1.03
973	0.91	6.54	71.9	0.73	802	30.8	78.3	1.02
973	0.91	6.54	71.9	0.91	1000	30.8	91.7	1.02
1073	0.96	6.52	67.9	0.45	469	32.1	84.4	1.01
1073	0.96	6.52	67.9	0.55	573	32.1	99.7	1.01
1073	0.96	6.52	67.9	0.72	750	32.1	107.2	1.01

summarized in Table 1, as well as the calculated stoichiometric factors f being in the range $1.08 \leq f \leq 1.23$. In Fig. 2 the first order rates at 6 different temperatures are plotted versus the C_2H_6 concentrations.

From a least-square treatment of the data in Table 1 the following Arrhenius temperature dependence of the rate constants in the above given temperature range is obtained:

$$k_1(T) = 9.7 \cdot 10^{12} \exp(-44.4 \pm 3 \text{ kJ mol}^{-1}/RT) [\text{cm}^3/\text{mol} \cdot \text{s}].$$

Within experimental error the Arrhenius plot was observed to be linear.

The Reaction of Amino Radicals with Propane

The experimental conditions and results for the reaction of NH_2 with C_3H_8



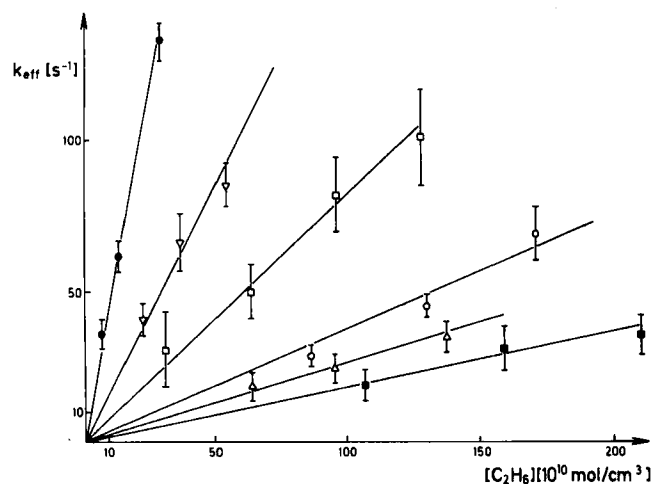


Fig. 2

Pseudo-first order rate constants as function of the C_2H_6 -concentration, $p = 4$ mbar, $0.9 \leq [\text{NH}_2]_0/10^{-12} \text{ mol/cm}^3 \leq 1.4$. T [K]
 ■ = 598, △ = 630, ○ = 673, □ = 743, ▽ = 823, ● = 973

are summarized in Table 2 for 21 runs at 7 different temperatures. The reaction was studied in the temperature range $550 \leq T/\text{K} \leq 1073$ at a pressure of $p = 4$ mbar, under pseudo-first order conditions of a large excess of $[\text{C}_3\text{H}_8]_0$ over $[\text{NH}_2]_0$ ($5 \cdot 10^2 \leq [\text{C}_3\text{H}_8]_0/[\text{NH}_2]_0 \leq 2 \cdot 10^4$). The stoichiometric factors were in the range $1.01 \leq f \leq 1.09$.

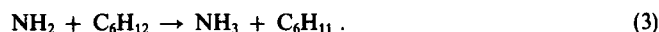
The data from Table 2 yield the following Arrhenius temperature dependence of the rate constants in the above given temperature range:

$$k_2(T) = 8.5 \cdot 10^{12} \exp(-39.3 \pm 4 \text{ kJ mol}^{-1}/RT) [\text{cm}^3/\text{mol} \cdot \text{s}] .$$

Despite the fact that there are two possible channels in the reaction of NH_2 with C_3H_8 the Arrhenius-plot in the above given temperature range was linear within the experimental error (see discussion).

The Reaction of Amino Radicals with Cyclohexane

Provided that ring breaking reactions are excluded because of the stability of the cyclohexane ring, the reaction of NH_2 with C_6H_{12} is an abstraction reaction:



The experimental results for this reaction are summarized in Table 3. At 6 temperatures in the temperature range $544 \leq T/\text{K} \leq 973$ at a pressure $p = 4$ mbar 16 runs were carried out. With an excess of $[\text{C}_6\text{H}_{12}]$ over $[\text{NH}_2]$ in the range $2 \cdot 10^2 \leq [\text{C}_6\text{H}_{12}]_0/[\text{NH}_2]_0 \leq 8 \cdot 10^3$ the stoichiometric factors were in the range $1.05 \leq f \leq 1.17$. From the data in Table 3 the following Arrhenius temperature dependence of the rate constants in the above given temperature range is obtained:

$$k_3(T) = 2.7 \cdot 10^{13} \exp(-37.3 \pm 5 \text{ kJ mol}^{-1}/RT) [\text{cm}^3/\text{mol} \cdot \text{s}] .$$

Within the experimental error no curvature of the Arrhenius plot was observed.

The results for $k_1(T)$, $k_2(T)$ and $k_3(T)$ are shown in Fig. 3 in an Arrhenius plot.

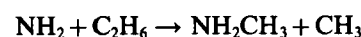
Discussion

Besides methane, ethane is the smallest hydrocarbon with only primary H atoms. There is only one exothermic reaction path in the reaction with NH_2 :



$$\Delta H_R(298 \text{ K}) = -42.5 \text{ kJ/mol}$$

since the product channel:



$$\Delta H_R(298 \text{ K}) = +13.0 \text{ kJ/mol}$$

is endothermic due to the higher energy of CH_3 compared to C_2H_5 .

Table 3
Experimental conditions and results for reaction (3)

T [K]	$[\text{NH}_2]_0 \cdot 10^{12}$ [mol/cm ³]	$\frac{[\text{NH}_3]}{[\text{F}_2]}$	$[\text{C}_2\text{H}_{12}]_0 \cdot 10^9$ [mol/cm ³]	$\frac{[\text{C}_6\text{H}_{12}]_0}{[\text{NH}_2]_0}$	k_w [s ⁻¹]	k_{ex} [s ⁻¹]	f
544	0.57	62	4.73	5120	19.1	51.3	1.17
544	0.57	62	6.49	7030	19.1	63.1	1.16
544	0.57	62	7.30	7900	19.1	72.7	1.15
573	1.03	56	5.04	5150	64.2	131.2	1.17
600	0.98	57	2.83	2950	48.6	102.7	1.10
600	0.98	57	3.80	4040	48.6	110.4	1.09
673	1.03	58	0.80	790	26.5	68.1	1.13
673	1.03	58	1.14	1130	26.5	73.9	1.12
673	1.03	58	1.60	1580	26.5	104.0	1.11
773	1.05	56	0.47	450	32.9	67.3	1.12
773	1.05	56	0.75	710	32.9	85.6	1.10
773	1.05	56	1.13	1090	32.9	124.2	1.09
973	1.05	60	0.18	200	23.3	87.4	1.10
973	1.05	60	0.33	370	23.3	141.4	1.08
973	1.05	60	0.52	590	23.3	146.6	1.07
973	1.05	60	0.69	770	23.3	234.7	1.05

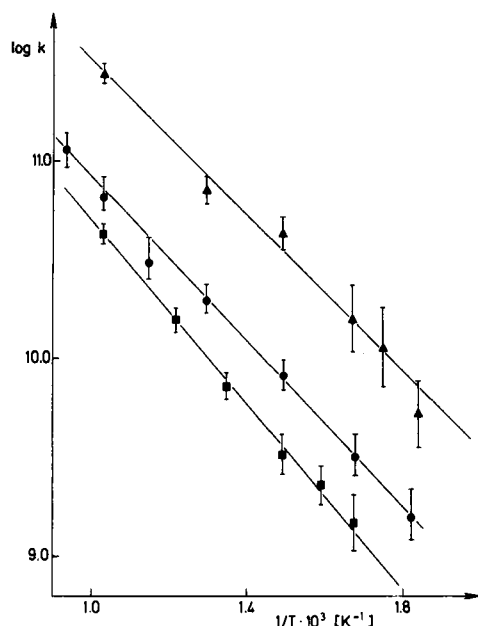


Fig. 3
Arrhenius-plot for reactions (1-3)
■: ethane, ▲: cyclohexane, ●: propane

For the rate of reaction (1) and its temperature dependence two studies have been published in the literature, a determination at low temperatures by Demissy and Lesclaux [11] and an indirect determination at higher temperatures by Rozenberg and Voronkov [3].

In the low temperature range $360 \leq T/\text{K} \leq 520$ an Arrhenius expression of $k_1(T) = 3.7 \cdot 10^{11} \exp(-29.9 \text{ kJ mol}^{-1}/RT) \text{ cm}^3/\text{mol} \cdot \text{s}$ was obtained in flash photolysis experiments [11]. The slope and the pre-exponential factor

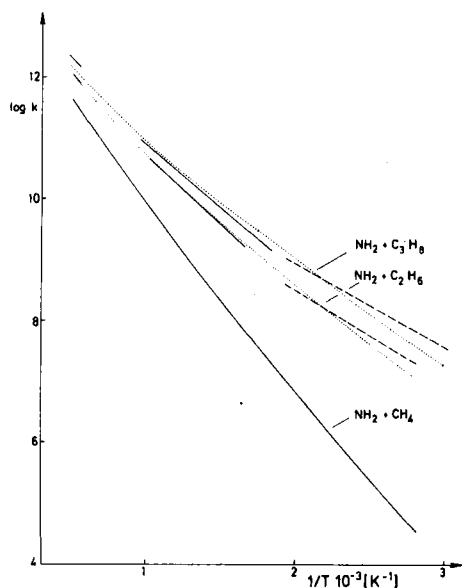


Fig. 4
Comparison of $k_1(T)$ and $k_2(T)$ measured at different temperatures. $1700 \leq T/\text{K} \leq 2200$ (Rozenberg 1972); — this work — — — (Demissy 1980). [$k_1(T) = 8.6 \cdot 10^{11} (T/700 \text{ K})^2 \exp(-29.5 \text{ kJ mol}^{-1}/RT) \text{ cm}^3/\text{mol} \cdot \text{s}$]. Reaction rate of $\text{NH}_2 + \text{CH}_4 \rightarrow \text{NH}_3 + \text{CH}_3$ in the temperature range $300 \leq T/\text{K} \leq 2000$

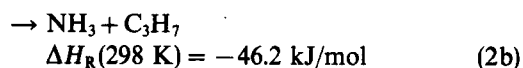
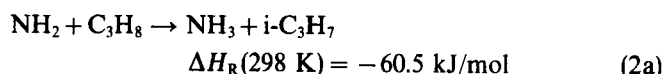
show some deviations in comparison with this work; whereas the absolute value at a medium temperature of $T = 500 \text{ K}$ differs only by about 30% (see Fig. 4).

An explanation for the deviations cannot be based on a stoichiometric factor, since the excess in the photolytic system was larger than $[\text{RH}]_0/[\text{NH}_2]_0 > 10^7$. The other significant difference between photolytic systems and flow systems is the wall effect which cannot be excluded in flow systems. In order to limit the relative error, due to the wall effect, to that amount caused by the possible change in k_w itself, only those values with $k_w < k_{\text{eff}}$ were finally taken into consideration. Photolytic systems on the other hand do have other problems.

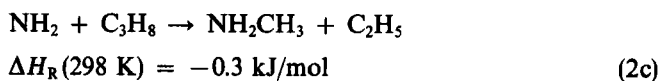
An explanation due to a deviation of $k_1(T)$ from the Arrhenius behaviour is discussed taking into account the high temperature values of Rozenberg and Voronkov [3], which were measured relative to the rate of the reaction $\text{NH}_2 + \text{CH}_4$. Using more recent high temperature data [12] of this reaction rate, an Arrhenius-expression $k_1(T) = 2.0 \cdot 10^{13} \exp(-47.6 \text{ kJ mol}^{-1}/RT) \text{ cm}^3/\text{mol} \cdot \text{s}$ results in the temperature range $1700 \leq T/\text{K} \leq 2000$.

The rate constants measured for $k_1(T)$ are summarized in Fig. 4. All data can possibly be explained by a curvature in the Arrhenius plot in the temperature range $360 \leq T/\text{K} \leq 2000$, thus it was tested, whether they could be described by an expression of the form $k(T) = A \cdot (T/T_0)^n \exp(-\alpha/T)$. The value of n however, to fit these three different sets of data, was unreasonable high. The dotted curve refers to $n = 2$. For comparison the data for the reaction $\text{NH}_2 + \text{CH}_4 \rightarrow \text{NH}_3 + \text{CH}_3$ are shown which are described by $k(T) = 8.5 \cdot 10^7 \cdot T^{1.5} \exp(-50 \text{ kJ mol}^{-1}/RT) \text{ cm}^3/\text{mol} \cdot \text{s}$ [5].

For the reaction



a primary as well as a secondary H atom can be abstracted by NH_2 , and also the substitution:



is slightly exothermic. Ignoring the substitution channel (2c) the measured rate constant for reaction (2) at any temperature can be composed of two different rates k_{2a} and k_{2b} which may have a different temperature dependence, since the bond energies for primary and secondary C-H bonds are different. In the temperature range $550 \leq T/\text{K} \leq 1073$ the Arrhenius-expression was found to be linear within experimental errors (see Fig. 3), despite these two possible different reaction channels. This fact can be explained by the assumption that at higher temperatures channel (2b), the less exothermic channel with six H atoms for abstraction, camouflages the part of channel (2a) with only two H atoms for abstraction. Channel (2a) should dominate at lower temperatures.

For the rate of reaction (2) and its temperature dependence one study has been published in the literature by De-

missy and Lesclaux [11]. In the low temperature range an Arrhenius expression of $k_2(T) = 4.5 \cdot 10^{11} \exp(-25.7 \text{ kJ mol}^{-1}/RT) [\text{cm}^3/\text{mol} \cdot \text{s}]$ was obtained.

A difficulty arises if the activation energy of reaction (2) is correlated with the C–H bond energy of propane because of the two different reaction channels (2a) and (2b) already described. The measured activation energy cannot be associated with one of the two reaction channels, because at each temperature the NH_2 radicals react along both pathways. The overall rate constant $k_2(T)$ should be of the form:

$$k_2(T) = k_{2a}(T) + k_{2b}(T) \\ = k_{0a} \exp(-E_{Aa}/RT) + k_{0b} \exp(-E_{Ab}/RT)$$

with $E_{Aa} < E_{Ab}$ and $k_{0a} < k_{0b}$.

A semiempirical correlation between the activation energy and the energy of the broken C–H bond can be used to discriminate the contribution of the two reaction channels. For a series of reactions of the same type, the Arrhenius activation energy E_A can be related to the reaction enthalpy ΔH_R [6].

$$E_A = \alpha \cdot \Delta H_R + C$$

where α and C are constants from a plot of E_A versus ΔH_R .

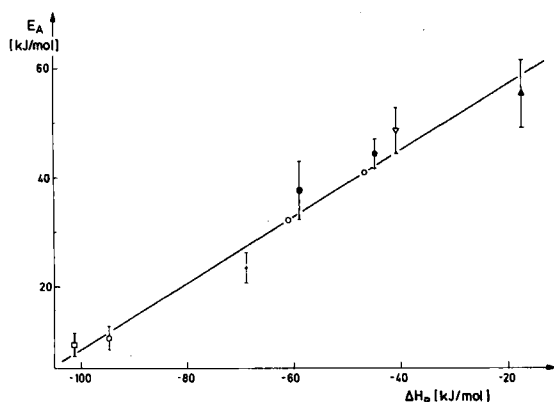


Fig. 5

Evans-Polanyi-plot. Experimental activation energies versus reaction enthalpy at medium temperatures of measurement. ▲: methane, ●: ethane, ○: propane, ▽: 2,2-dimethylpropane, +: iso-butane, ■: cyclohexane, ○: acetaldehyde, □: toluene

A plot of E_A versus ΔH_R for several H atom abstraction reactions with NH_2 radicals [13] is shown in Fig. 5. All C–H bond energies have been taken from a recent review [14], together with all other data they are summarized in Table 4.

The ΔH_R values for reaction (2a) and (2b) are correlated with the activation energies $E_{Aa} = 32 \text{ kJ/mol}$ and $E_{Ab} = 41 \text{ kJ/mol}$. Thus the following expression:

$$k_2(T) = 7 \cdot 10^{11} \exp(-32 \text{ kJ mol}^{-1}/RT) \\ + 7 \cdot 10^{12} \exp(-41 \text{ kJ mol}^{-1}/RT) \text{ cm}^3/\text{mol} \cdot \text{s}$$

can then be obtained over the temperature range $300 \leq T/\text{K} \leq 1073$.

Table 4

Experimental Arrhenius-activation energies E_A (kJ/mol), reaction enthalpies and bond energies $D(\text{RH})$ [kJ/mol] at a medium temperature T . $D(\text{R-H})$ values for room temperature were taken from Ref. [14] and were converted to T with $c_p(T)$ -values from the literature or from group additivity rules [21]. Standard formation enthalpies used in this work: ΔH_f [kJ/mol] C_2H_6 : -84.5, C_2H_5 : 110.9, C_3H_8 : -103.8, $n\text{-C}_3\text{H}_7$: 87.9, $i\text{-C}_3\text{H}_7$: 73.6, C_6H_{12} : -122.6, C_6H_{11} : 54.4, NH_3 : -45.9, NH_2 : 192.0, CH_3 : 143.5, $\text{NH}_2\text{-NH}_2$: -23.0, $\text{CH}_2\text{-NH}_2$: 140.2, $\text{NH}_2\text{-(CH}_2)_5\text{-CH}_2$: 59.7

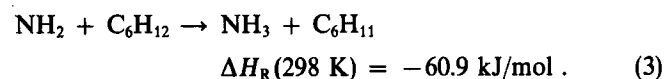
	T [K]	$D(\text{RH})$ [kJ/mol]	$\Delta H_{R,T}$ [kJ/mol]	E_A [kJ/mol]	References
CH_4	880	450 ± 1	-17.5	55.1 ± 6	[4]
C_2H_6	785	415 ± 4	-44.6	44.4 ± 3	this work
C_3H_8	330	398 ± 4	-60.5	32	this work
		410	-46.2	41	this work
$i\text{-C}_4\text{H}_{10}$	470	392 ± 8	-60.8	22 ± 2	[5]
$\text{neo-C}_3\text{H}_{12}$	840	424 ± 8	-40.9	48.6 ± 4	[5]
C_6H_{12}	760	406 ± 4	-59.0	37.3 ± 5	this work
toluene	425	369 ± 4	-94.7	9.4 ± 2	[5]
CH_3CHO	420	360 ± 3	-101.3	10.4 ± 2	[5]

As shown for CH_4 and C_2H_6 for a larger temperature range the deviation from a Arrhenius-type approximation has to be taken into account. This is demonstrated with an expression:

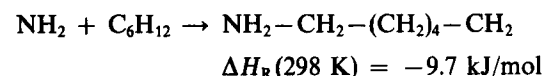
$$k_2(T) = 1.4 \cdot 10^{12} \exp(-32/RT) \\ + 2.0 \cdot 10^{12} (T/T_0)^{1.5} \exp(-34/RT) \text{ cm}^3/\text{mol s}$$

in Fig. 4 for the temperature range $300 \leq T/\text{K} \leq 2000$ with $T_0 = 700 \text{ K}$. This expression, taking a somewhat higher activation for the primary H atoms, brings the values measured in the temperature range of this work and those measured at low temperatures [11] in good agreement. For the term $(T/T_0)^n$ the same value of n was chosen as for the reaction of NH_2 with the primary H atoms of CH_4 . A better agreement with the high temperature values [3] could be obtained with $n > 1.5$.

For the reaction NH_2 with cyclohexane there is only one expected path:

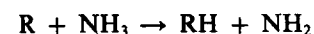


A decomposition of the cyclohexane ring into open-chain fragments like:



during the reaction with NH_2 is unlikely under the experimental conditions, mainly because the ring is free of tension. Thus the activation energy of $E_A = 37.3 \text{ kJ/mol}$ can be correlated with only one possible H atom abstraction.

The reactions of the hydrocarbon radicals with ammonia:



are all endothermic and may occur at higher temperatures. The rates calculated from the reverse reactions using the

value for the heat of formation of NH_2 determined recently are:

$$k_{-1}(T) = 3.8 \cdot 10^{12} \exp(-88.6 \text{ kJ mol}^{-1}/RT) \text{ cm}^3/\text{mol s}$$

$$k_{-2}(T) = 3.2 \cdot 10^{11} \exp(-89.0 \text{ kJ mol}^{-1}/RT) \text{ cm}^3/\text{mol s}$$

and

$$k_{-3}(T) = 1.5 \cdot 10^{12} \exp(-95.9 \text{ kJ mol}^{-1}/RT) \text{ cm}^3/\text{mol s}$$

in the temperature range $500 \leq T/\text{K} \leq 1000$.

Comparison with the Reactions of Isolelectronic Radicals

For the $\text{OH}(\text{X}^2\Pi)$ radical many hydrocarbon reactions have been studied [15,16], to a less extent this applies to reactions of $\text{CH}_3(\tilde{\text{X}}^2\text{A}_2')$ radicals [17,18]. For both radicals there are more kinetic data available than for the $\text{NH}_2(\tilde{\text{X}}^2\text{B}_1)$ -radical.

Generally it can be said that hydrogen abstraction reactions from hydrocarbons by OH radicals proceed rather rapidly with low activation energies, whereas the comparable CH_3 reactions are significantly slower and require larger activation energies. Considerations based on theoretical grounds suggest a similar curvature in the Arrhenius plots of the three radicals OH, NH_2 and CH_3 . Recent results [19,20] indicate a curvature in the Arrhenius plots for the reactions of OH with C_2H_6 and C_3H_8 . It is seen from the absolute values that the reaction rates of NH_2 with the reported hydrocarbons are in an intermediate range. The following well established order

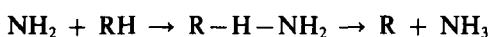
$$k[\text{OH}(\text{X}^2\Pi)] \gg k[\text{NH}_2(\tilde{\text{X}}^2\text{B}_1)] > k[\text{CH}_3(\tilde{\text{X}}^2\text{A}_2')]$$

can be given for the reactivity of the radicals in their electronic ground states.

Semi-Empirical Predictions of the Activation Energies for NH_2 -Reactions with Further Saturated Hydrocarbons

One method to predict kinetic data of H atom abstraction reactions of NH_2 radicals from hydrocarbons is a plot of E_A , measured for a variety of hydrocarbons, versus ΔH_R of these reactions, as shown in Fig. 5. Another method, which can be used for this purpose is the semi-empirical bond-energy-bond-order (BEBO) method which allows the calculation of activation energies of atom-transfer-reactions from known molecule parameters [21].

The reaction:



is described by a progress variable n_{RH} in the range $0 \leq n_{\text{RH}} \leq 1$, where n_{RH} means the bond-order of the bond being broken. A detailed description of the calculation used here is reported elsewhere [5], so only the results are shown here. They are summarized together with the necessary molecular parameters in Table 5.

The deviations of the calculated activation energies from the experimental values are considerable, up to about 40%

Table 5

Parameter used for BEBO-calculations.

D_{RH} : bond energy at a medium temperature T , (a) from Ref. [14] (b) from Ref. [13]; r : bond length from Ref. [22]; vibrational frequencies from Ref. [23], $E_A(\text{cal})$: activation energy calculated with the BEBO-method; $E_A(\text{ex})$: experimental activation energy

		C_2H_6	C_3H_8	C_6H_{12}
T	[K]	785	330	760
D_{CH} (a)	[kJ/mol]	415.9	398.3	406.3
D_{NH} (b)	[kJ/mol]	462.0	455.0	461.7
D_{CN} (c)	[kJ/mol]	364.0	346.0	363.9
r_{CH}	[Å]	1.095	1.073	1.095
r_{NH}	[Å]	1.1	1.1	1.1
r_{CN}	[Å]	1.47	1.47	1.47
ω_{CH}	[cm ⁻¹]	2955	2876	2930
ω_{NH}	[cm ⁻¹]	3390	3390	3390
ω_{CN}	[cm ⁻¹]	1079	1041	1075
$E_A(\text{cal})$	[kJ/mol]	27.9	21.6	24.8
$E_A(\text{ex})$	[kJ/mol]	44.4	39.3	37.3

(This discrepancy could be explained by the poor accuracy of some molecular parameters involved in the calculation or, more probably, by the fact that the measurements were conducted at higher temperatures, whereas the BEBO-method was applied up to now only to measurements at lower temperatures). Nevertheless the calculated E_A values are useful to predict E_A values of unknown reaction rates. A plot of $E_A(\text{cal})$ versus $E_A(\text{ex})$ for e.g. CH_4 , C_2H_6 , C_3H_8 and neo- C_5H_{12} yields a straight line, and although other hydrocarbons do not fit exactly to that line, such a plot can be used for a "prediction" of an unknown activation energy. The activation energies obtained from the Evans-Polanyi- and such BEBO-plot can be given with a 20% confidence for a given temperature range, taking into account that the effective activation energies are temperature dependant. With these prediction methods, the kinetic data measured for selected specific reactions are fit for supporting points for the whole field of reactions of the same type.

Financial support of the Fonds der Chemie is acknowledged. One of the authors (R.R.) expresses thanks for a scholarship of the Max-Planck Society.

References

- [1] B. S. Haynes, Comb. Flame 28, 81 (1977).
- [2] R. Lesclaux, Rev. Chem. Intermed. 5, 347 (1984).
- [3] A. S. Rozenberg and V. G. Voronkov, Russ. J. Phys. Chem. 46, 425 (1972).
- [4] W. Hack, H. Kurzke, R. Rouveiolles, and H. Gg. Wagner, 21st Combustion Symposium (accepted for publication, Munich 1986).
- [5] W. Hack, H. Kurzke, P. Rouveiolles, and H. Gg. Wagner, Ber. Bunsenges. Phys. Chem. 90, 1210 (1986).
- [6] M. G. Evans and M. Polanyi, Trans. Faraday Soc. 34, 11 (1938).
- [7] W. Hack, O. Horie, and H. Gg. Wagner, J. Phys. Chem. 86, 765 (1982).
- [8] M. Kroll, J. Chem. Phys. 63, 319 (1975).
- [9] R. Lesclaux and M. Demissy, J. Photochem. 9, 110 (1978).
- [10] M. Demissy and R. Lesclaux, Int. J. Chem. Kinet. 14, 1 (1982).
- [11] M. Demissy and R. Lesclaux, J. Am. Chem. Soc. 102, 2897 (1980).
- [12] W. Möller and H. Gg. Wagner, Z. Naturforsch. 39a, 846 (1984).

- [13] W. Hack, P. Rouveirolles, and H. Gg. Wagner, *J. Phys. Chem.* **90**, 2505 (1986).
 [14] D. F. McMillen and D. M. Golden, *Ann. Rev. Phys. Chem.* **33**, 493 (1982).
 [15] K. M. Jeong and F. Kaufman, *J. Phys. Chem.* **86**, 1808 (1982).
 [16] R. Atkinson, *Chem. Rev.* **86**, 69 (1986).
 [17] W. Möller, E. Mozzhukhin, and H. Gg. Wagner, *Ber. Bunsenges. Phys. Chem.*, in press 1987.
 [18] P. Gray, A. A. Herod, and A. Jones, *Chem. Rev.* **71**, 247 (1971).
 [19] F. P. Tully, A. T. Droege, M. L. Koszykowski, and C. F. Melius, *J. Phys. Chem.* **90**, 691 (1986).
 [20] A. T. Droege and F. P. Tully, *J. Phys. Chem.* **90**, 1949 (1986).
 [21] S. W. Benson, "Thermochemical Kinetics", 2nd Ed., A. Wiley Interscience Publication 1976.
 [22] R. D. Gilliom, *J. Am. Chem. Soc.* **99**, 8399 (1977).
 [23] *Handbook of Chemistry and Physics*, 55th Ed., CRC Press Inc. 1975.
 [24] G. Herzberg, *Molecular Spectra and Molecular Structure*, III, Van Nostrand Reinhold Comp., New York 1966.

(Eingegangen am 20 März 1987)

E 6469

Kinetics, Energetics and OH Product Yield of the Reaction $\text{CH}_3\text{O} + \text{O}(^3\text{P}) \rightarrow \text{CH}_3\text{O}_2^* \rightarrow \text{Products}$

F. Ewig, D. Rhäsa, and R. Zellner

Institut für Physikalische Chemie, Universität Göttingen, Tammannstraße 6, 3400 Göttingen

Chemical Kinetics / Elementary Reactions / Laser Induced Fluorescence / Reactions with Bound Intermediates / Radicals

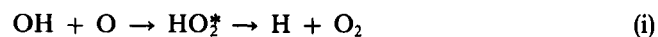
The rate constant for the reaction (1) $\text{CH}_3\text{O} + \text{O} \rightarrow \text{products}$ at 298 K has been determined using 248 nm laser co-photolysis of $\text{CH}_3\text{ONO}/\text{O}_3$ mixtures for the generation of CH_3O radicals and O atoms combined with LIF for time resolved detection of CH_3O and product OH. k_1 is found to be $(2.5 \pm 0.7) \cdot 10^{-11} \text{ cm}^3/\text{s}$ with a relative yield of OH of $\varphi = -\Delta[\text{OH}]/\Delta[\text{CH}_3\text{O}] = 0.12 \pm 0.08$. The results are shown to be consistent with a primary capture mechanism on an electronically adiabatic surface forming highly vibrationally excited CH_3O_2^* and followed by rapid subsequent decomposition or isomerization, viz.



From modelling of the OH yield using RRKM theory the isomerization barrier between CH_3O_2 and CH_2OOH is placed near 160 kJ/mol in good agreement with recent ab initio calculations. As a consequence the $\text{CH}_3 + \text{O}_2$ combustion reaction is predicted to proceed primarily via the low energy $\text{CH}_2\text{O} + \text{OH}$ channel, in contrast to most previous suggestions.

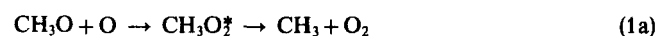
I. Introduction

In conventional terms bimolecular reactions are characterized by the existence of more or less pronounced potential energy barriers between reactants and products. Some of them, however, occur on purely attractive potentials like termolecular recombination processes and gain their bimolecular nature via the strong forward flux caused by the unimolecular fragmentation of the excited adducts. A notable example is the reaction



which in a number of experimental [1–3] and theoretical [3–5] studies has been shown to bear all properties of a recombination reaction in the high pressure limit.

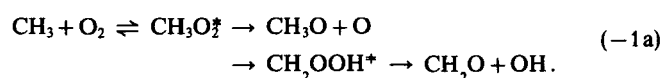
In the present paper we report an experimental and computational study of the reaction



This reaction is the simplest hydrocarbon analogue of reaction (i). Moreover, both reactions have strong energetic similarities through the intermediate formation of the per-

oxy species. As a consequence one may hope that similarities or differences between the rate coefficients of (i) and (1) can be extracted and be rationalized on the basis of current rate theory. An application of this approach to the reverse reactions, (–i) $\text{H} + \text{O}_2 \rightleftharpoons \text{HO}_2^* \rightarrow \text{OH} + \text{O}$ and (–1a) $\text{CH}_3 + \text{O}_2 \rightleftharpoons \text{CH}_3\text{O}_2^* \rightarrow \text{CH}_3\text{O} + \text{O}$, has recently been published by Cobos et al. [5, 6].

The hydrocarbon reaction (1) differs from reaction (i) through the existence of at least one additional exothermic reaction channel, i.e. the isomerization of CH_3O_2^* to CH_2OOH^* via 1,4-H-atom migration followed by subsequent decomposition of CH_2OOH to yield $\text{CH}_2\text{O} + \text{OH}$ (channel 1b). The branching ratio of this channel is a function of the height of the isomerization barrier ΔE_{iso} . This quantity is also of fundamental importance to the $\text{CH}_3 + \text{O}_2$ chain branching reaction at high temperatures, viz.



Although there is a large amount of experimental data on reaction (–1a) (for a summary see Ref. [7]) there is still conflicting evidence as to the branching ratio into the $\text{CH}_2\text{O} + \text{OH}$ channel. Arrhenius expressions for this channel with